Journal of Translational Medicine

RESEARCH

Open Access

SOX4 accelerates intervertebral disc degeneration via EZH2/NRF2 pathway in response to mitochondrial ROS-dependent NLRP3 inflammasome activation in nucleus pulposus cells

Wenzhi Zhao[1], Yadong Liu[2], Yunxiang Hu[2] and Guiqi Zhang[2*]

Abstract

Objective The transcription factor SRY-related HMG-box 4 (SOX4) has been implicated in intervertebral disc diseases. This study aimed to investigate the role of SOX4 in intervertebral disc degeneration (IDD) and explore the underlying molecular mechanisms.

Methods We established an IDD rat model via surgery and analyzed SOX4 expression using qRT-PCR and Western blotting. Histological evaluation, immunohistochemistry, and Safranin O staining assessed IDD progression. In vitro, an IDD cellular model was constructed using IL-1β-stimulated nucleus pulposus (NP) cells. SOX4 knockdown and overexpression experiments in NP cells examined SOX4 effects on ECM degradation, NLRP3-mediated pyroptosis, and mitochondrial ROS-dependent NLRP3 inflammasome activation. The involvement of the EZH2/NRF2 pathway in SOX4-mediated NLRP3 activation was also examined.

Results SOX4 expression was significantly increased in IDD rats and promoted IDD progression. Knockdown of SOX4 inhibited ECM degradation and NLRP3-mediated pyroptosis in NP cells. In vitro experiments showed that SOX4 promoted ECM degradation by upregulating MMPs and ADAMTS-5 expression, and suppressed collagen II and aggrecan synthesis. SOX4 knockdown inhibited NLRP3-mediated pyroptosis, while overexpression accelerated it in NP cells. Additionally, SOX4 was found to exacerbate mitochondrial ROS-dependent NLRP3 inflammasome activation in NP cells. Further investigation revealed that SOX4 enhanced NLRP3 inflammasome activation by upregulating EZH2 expression and modulating the EZH2/NRF2 pathway, with EZH2 inhibition attenuating SOX4-induced NLRP3 activation.

Conclusion Our findings suggest that SOX4 accelerates IDD progression by promoting NLRP3 inflammasome activation via modulating the EZH2/NRF2 pathway, leading to NP cell pyroptosis and ECM degradation. Targeting SOX4 may represent a potential therapeutic strategy for treating IDD.

*Correspondence:
Guiqi Zhang
93009950@qq.com

Full list of author information is available at the end of the article

Keywords SRY-related HMG-box 4, Intervertebral disc degeneration, EZH2/NRF2 pathway, NLRP3 inflammasome activation, Extracellular matrix degradation, Pyroptosis

Introduction

Intervertebral disc degeneration (IDD) is a widespread degenerative disorder of the musculoskeletal system, significantly contributing to chronic low back pain and affecting patients' quality of life. IDD, a principal cause of back pain, is estimated to affect about 80% of people during their lifetime [1]. Currently, the treatment options for IDD primarily focus on symptomatic relief and conservative management. However, none of these treatments have successfully slowed or reversed the degenerative process [2], urging to develop better and more effective therapeutics. Surgical interventions, including intervertebral disc removal and spinal fusion, are commonly relied upon. However, these procedures often fail to deliver long-term therapeutic benefits [3]. Therefore, it is essential to persistently explore the new therapeutic interventions to improve the outcomes of IDD.

The impairment of nucleus pulposus (NP) cells and the degradation of the extracellular matrix (ECM) constitute critical features in IDD [4, 5]. In IDD, mechanical loading may induce ECM damage, contributing to an abnormal NP cell microenvironment [6]. Moreover, NP cell aging is associated with organelle dysfunction, especially in mitochondria [7]. IDD can lead to mitochondrial dysfunction in NP cells [8]. Mitochondrial dysfunction triggers the generation of reactive oxygen species (ROS), subsequently causing heightened inflammation, disrupted metabolism, and increased apoptosis in cells [9]. Mitochondrial ROS activates the NLRP3 inflammasome, known for its detrimental role in IDD [10]. NLRP3 inflammasome can promote pyroptosis in NP cells during IDD progression, accelerating ECM degradation [11, 12]. NLRP3 inflammasome activation increases IL-1β production, promoting metalloproteinase secretion and leading to NP tissue degradation [13]. Therefore, the mitochondria ROS-dependent activation of NLRP3 inflammasomes in NP cells plays a pivotal role in regulating IDD homeostasis.

SRY-related HMG-box 4 (SOX4) represents an intronless gene encoding for a member of the SOX transcription factor family [14, 15]. Previous studies have revealed that SOX4 can promote inflammatory response and activate NLRP3 inflammasomes [16, 17]. Moreover, aberrant SOX4 expression in NP cells induces apoptosis, thereby accelerating IDD development [18, 19]. SOX4 regulates ECM degradation, influencing intervertebral disc structure and function, thereby affecting IDD progression [20, 21]. Although these findings suggest a role for SOX4 in IDD treatment, its precise mechanism of action remains elusive. Recent studies reported that SOX4 can regulate EZH2 in various diseases [22, 23]. EZH2 is known to promote cartilage endplate degeneration and IDD progression [24, 25]. The upregulation of EZH2 can induce inflammasome activation and ROS production by suppressing NRF2 expression [26]. Moreover, it has been reported that activation of the NRF2 signaling pathway can facilitate IDD treatment [27]. Therefore, we hypothesize that SOX4 may modulate the NRF2 pathway through EZH2, in response to mitochondrial ROS-dependent activation of NLRP3 inflammasomes in NP cells, promoting IDD progression.

In this study, we used in vivo and in vitro IDD models to explore the role of SOX4 on NP cell pyroptosis, mitochondrial dysfunction, and ECM degradation. Additionally, we investigated the potential relationship of SOX4 with the EZH2/NRF2 pathway. Our research provides a comprehensive analysis and deeper understanding of the role of SOX4 in IDD progression and the therapeutic possibilities it might offer.

Methods

Animal model and treatment

Twenty-four male Lewis rats (13–14 weeks old, weighing 450 ± 50 g), obtained from College of Veterinary Medicine Yangzhou University, were used in this study. The rats were kept under a 12-h light/dark cycle, at a controlled temperature of 23 °C, with free access to food and water. Yangzhou University's Animal Ethics Committee approved all experimental protocols (approval number: 202306014).

Initially, rats were anesthetized using an intraperitoneal injection of sodium pentobarbital (30 mg/kg). After being anesthetized, the animals were set in a prone position. A midline dorsal incision was then made to reveal the C6-C7 and C8-C9 intervertebral discs. An 18 G needle was carefully inserted into the discs to a depth of 5 mm. Upon complete insertion, the needle was rotated 360° and held in that position for 20 s. The control group underwent exposure of intervertebral discs without puncture. After the puncture procedure was completed, 3 μL of negative control (NC), sh-SOX4 (5'-GCCGGTCT GTTGCATGCAA-3'), or oe-SOX4 was injected into the nucleus pulposus (NP) tissue core using a 27 G microsyringe two weeks later. Following eight weeks of treatment, the rats were euthanized using 7.5% isoflurane inhalation. The NP tissues and blood samples were then harvested for further studies.

Magnetic resonance imaging (MRI)

MRI was performed to assess the signal and structural changes of discs in sagittal T2-weighted images with a 7T clinical magnet (BioSpec 70/20USR, Bruker) at 0 week and 8 weeks after surgery. The parameters of T2-weighted imaging were referenced as a previous publication [28]: TR = 2000 ms, andTE = 28.64 ms. The MRI images were evaluated according to the Pfirrmann grading scale and the mean gray value of all pixels in the NP area was measured by ImageJ.

Pfirrmann scoring criteria were divided five grades: Grade I: the nucleus pulposus of the intervertebral disc showed uniform high signal, clear boundary with the annulus fibrosus, and normal vertebral space height; Grade II: the nucleus pulposus of the intervertebral disc showed uneven high signal, the nucleus pulposus had or did not have horizontal low signal bands, the boundary between the nucleus and the annulus fibrosus was clear, and the vertebral space height was normal; Grade III: the nucleus pulposus of the intervertebral disc presents an uneven medium signal, the boundary with the fibrous annulus is not clear, and the height of the vertebral space is normal or slightly reduced. Grade IV: uneven moderate or low signal in the nucleus pulposus of the intervertebral disc, indistinguishable nucleus pulposus from annulus fibrosus, normal or moderately reduced vertebral space height; Grade V: the nucleus pulposus of the intervertebral disc shows uneven low signal, indistinguishable from the annulus fibrosus, and the vertebral space is severely narrowed.

Histological examination

The NP tissue was stained with hematoxylin-eosin (HE) [29]. Briefly, samples were fixed in 4% paraformaldehyde for 24 h. After the processed, samples were embedded in paraffin and cut into 4–7 μm. Standard HE staining was used to examine tissue histology. The sections were stained with a haematoxylin solution for 5 min and then were stained with an eosin solution for 1–2 min. Safranin O and fast green staining was performed to determine changes in proteoglycans. The sections were stained with a Safranin O staining kit (G1371, Solarbio) according to the manufacturer's recommended procedure. Briefly, sections were stained with Weigert solution for 3–5 min, and then stained with fast green solution for 5 min.

Immunohistochemistry

Samples sections were then deparaffinized and rehydrated in an oven at 60 ℃ for 2 h. After baking, the slices were dewaxed and hydrated using xylene and different concentrations of alcohol. Following deparaffinization, the slices underwent antigen retrieval using citrate repair solution. The endogenous peroxidase activity was blocked using 3% H_2O_2 solution. Then, sections were pre-treated with normal goat serum working fluid for 15 min. After pre-treatment, the sections were incubated with primary antibodies, including anti-ADAMTS-5 (dilution 1:1000; Thermo, MA, USA; PA5-32142), anti-MMP-13 (5 μg/mL dilution; Affinity, OH, USA; AF5355), and anti-caspase-3 (dilution 1:1000; Abcam, UK; ab184787), at 4℃ overnight. Following primary antibody incubation, the sections were incubated with secondary antibody (dilution 1:2000; Abcam; ab205718) for 15 min. Lastly, the sections were stained with DAB chromogen, counterstained with hematoxylin, dehydrated, cleared, and coverslipped for observation under an optical microscope (Olympus, Japan).

NP cells isolation, culture and treatment

NP tissue was carefully dissected under sterile conditions with the aid of a dissecting microscope and then digested at 37 °C for 2 h using 0.5% type II collagenase (Gibco). The digested tissue was cultured in DMEM/F-12 medium (Gibco) enhanced with 10% fetal bovine serum (FBS; Gibco), maintained at 37 °C within a 5% CO_2 humidified atmosphere. Cells were passaged using 0.25% trypsin-EDTA (Thermo Fisher Scientific) and re-seeded in a 10-cm culture dish at an optimal density. For subsequent experiments, NP cells from the first three generations were used. These included treatment with IL-1β (50 ng/mL; R&D Systems, MN, USA) for 24 h to mimic the in vitro IDD model, transfection with sh-NC, sh-SOX4, oe-SOX4 and oe-EZH2, or pre-treatment with Mito-tempo (a mitochondrial ROS inhibitor) for 2 h to inhibit mitochondrial ROS, NRF2 inhibitor ML385 (1 μM), or NRF2 activator sulforaphane (5 μM) for 1 h. The viability of the cells was ascertained using a CCK-8 kit (Beyotime, Shanghai, China) following the manufacturer's guidelines.

Cell apoptosis

Firstly, 5×10^4 cells were resuspended and resuspended in 195 μL of Annexin V-EGFP binding buffer. Subsequently, the cells were treated with 5 μL of Annexin V-EGFP and 10 μL of propidium iodide staining solution, followed by a 20-minute incubation at 25℃, shielded from light. Lastly, a flow cytometer (Beckman, CA, USA) was utilized for the analysis of cells in each tube.

Immunofluorescence

Cells were fixed using a 3% formaldehyde for 10 min and then permeabilized with 1% Triton-X 100 for 5 min. Following this, the samples are blocked with 3% BSA for 30 min. The primary antibodies, diluted at 1:100 for NLRP3 (Affinity, DF7438), 1:200 for GSDMD (Affinity, AF4012), 1:100 for MMP13, 1:50 for SOX4 (Thermo, PA5-72852), and 1:50 for EZH2 (Bioss, Beijing, China; bsm-60001R) are added to the cells, which are then

placed in a humidity chamber and incubated overnight at 4℃. For secondary antibody incubation and nuclear staining, Cy3-labeled goat anti-rabbit IgG (H + L; Beyotime, A0516) diluted at 1:200 or goat anti-rabbit IgG H&L (Alexa Fluor® 488; Abcam, ab150077) diluted at 1:500 and DAPI are added and incubated for 30 min at room temperature in the dark. The cells are then mounted using a fluorescence quenching sealant and sealed with nail polish. The cells are finally observed under a laser confocal scanning microscope (Zeiss, Germany).

Transmission electron microscopy (TEM)

Post 24 h treatment, cells were scraped, centrifuged and immediately fixed in a solution of glutaraldehyde. Following fixation, the cells were fixed in 1% osmium tetroxide for 2 h at 4℃. Then, cells were dehydrated at room temperature using acetone solutions, progressively increasing the concentration from 50 to 100%. Following dehydration, cells were infiltrated with a 1:1 mixture of acetone and EPON812 for 30 min. The sample was then embedded in a mold using the same mixture, baked at 60℃ for 2 h, mounted onto a trimming device, and excess embedding agent was removed under a microscope. Semi-thin sections of about 1 μm were cut, stained with toluidine blue, and examined under a microscope to determine the area for ultrathin sectioning. A cleaned copper mesh grid was prepared, and ultrathin sections of 70 nm were cut, picked, and pasted onto the grid. Finally, sections were stained with sodium acetate, washed, and air-dried for final observation.

ELISA

According to the instructions of the ELISA kits, the levels of MMP-1 (Solarbio, Beijing, China; SEKR-0065), MMP-2 (Solarbio, SEKR-0066), TIMP-1 (Solarbio, SEKR-0031), and TIMP-2 (Jianglai Biological, Shanghai, China; JL11383) in the supernatant of the NP tissue were measured. The 8-Hydroxydeoxyguanosine (8-OHdG) level in NP cells was detected using the 8-OHdG ELISA Kit (Elabscience, Wuhan, China; E-EL-0028).

JC-1 assay

In order to evaluate changes in mitochondrial membrane potential (ΔψM) using the JC-1 mitochondrial membrane potential assay kit (Beyotime, C2006), cells were cultured in 6-well plates at a seeding density of 3×10^5 cells per well. The assessment was conducted when they achieved a confluence of approximately 70%.

Dihydrodichlorofluorescein diacetate (H2DCF-DA) assay

NP cells were transfected with 10 μM H_2DCF-DA staining solution using the Reactive Oxygen Species Assay Kit (Solarbio, CA1410) in a 24-well plate (1×10^4 cells/well), incubated at 37 °C for 30 min. The images were captured on a fluorescence microscope (Olympus, Japan).

MitoSOX staining

To extract mitochondria for the MitoSOX assay, cells were digested using trypsin and then resuspended in 1 mL of mitochondria isolation reagent (Thermo). The suspension was incubated on ice for 10 min, followed by approximately 20 rounds of homogenization. The supernatant was transferred to another centrifuge tube and spun at 11,000 *g* for 10 min at 4℃, leaving behind a pellet of isolated mitochondria.

For the MitoSOX assay, samples were washed twice with D-Hank solution before being incubated with 1 mL of 5 μM MitoSOX working solution at 37℃ in the dark for 10 min. After washing three times with D-Hank solution, 1 mL of D-Hank solution was added to each well, and the samples were observed and photographed under an inverted fluorescence microscope (Olympus, Japan).

Chromatin immunoprecipitation (ChIP)-qRT-PCR

NP cells at 80% confluence were crosslinked using formaldehyde and quenched with 10× glycine. Cells were lysed with SDS lysis buffer and sonicated, and supernatant was collected post-centrifugation. The supernatant was incubated with SOX4 specific antibody (Thermo, PA5-72852) or rabbit IgG antibody (ABconal, AC005) for control, along with ChIP dilution buffer overnight at 4 °C. Protein A/G agarose beads were added and incubated for 1 h at 4 °C. Elution of bound material was done using the elution buffer for 20 min. The DNA-protein crosslinks were reversed using 5 M NaCl and further processed with RNase A, Proteinase K, 0.5 M EDTA, and 1 M Tris-HCl. The resulting solution was treated with Tris-saturated phenol, phenol/chloroform, and 3 M NaAc with twice the volume of anhydrous ethanol. Purified DNA was obtained and used for quantitative real-time PCR (qRT-PCR) analysis.

qRT-PCR

Using TRIzol reagent (Invitrogen), total RNA was extracted, with the concentration and purity assessed by a NanoDrop spectrophotometer (Thermo). The SuperScript IV Reverse Transcriptase Kit (Invitrogen) was employed to synthesize cDNA from the obtained RNA. Specific primers for the target genes, along with a GAPDH gene as a reference, were used to perform qRT-PCR analysis on a CFX96 Touch Real-Time PCR System (Bio-Rad, CA, USA). The qRT-PCR reaction was initiated using the PowerUp SYBR Green Master Mix (Applied Biosystems) with cycling conditions as follows: an initial 95℃ for 3 min, followed by 40 cycles of 95℃ for 12 s and 62℃ for 40 s. Relative mRNA expression levels of the target genes were estimated utilizing the $2^{-\Delta\Delta Ct}$ method and

Table 1 The prime sequences for qRT-PCR

Genes	Prime sequences(5′-3′)	Length(bp)
Col II forward	TCAGGAATTTGGTGTGGACATA	178
Col II reverse	CCGGACTGTGAGGTTAGGATAG	
Aggrecan forward	CTCTGGGATCTATCGGTGTGA	131
Aggrecan reverse	CTCGGTCAAAGTCCAGTGTGT	
MMP-13 forward	TCCATCCCGAGACCTCATGT	148
MMP-13 reverse	CTCAAAGTGAACCGCAGCAC	
iNOS forward	TCTTCGGTGCGGTCTTTTCC	70
iNOS reverse	AGTCTTGTGCCTTTGGGCTC	
COX-2 forward	GGTGAAAACTGTACTACGCCGA	645
COX-2 reverse	GACGTGGGGAGGGTAGATCA	
ADAMTS-5 forward	AGTACAGTTTGCCTACCGCC	222
ADAMTS-5 reverse	AGGACACCTGCGTATTTGGG	
SOX4 forward	TATGGTGTGGTCGCAGATCG	981
SOX4 reverse	GCGGATGAGGAGCTGAAACT	
EZH2 forward	AGGACGGCTCCTCTAACCAT	699
EZH2 reverse	TTTCTCGTTCGATGCCCACA	
Nrf2 forward	GTCCCAGCAGGACATGGATT	378
Nrf2 reverse	GGTGAAGAAACCTCATGGTCATC	
NLRP3 forward	ACGGCAAGTTCGAAAAAGGC	502
NLRP3 reverse	AGACCTCGGCAGAAGCTAGA	
GAPDH forward	GCGAGATCCCGCTAACATCA	178
GAPDH reverse	CTCGTGGTTCACACCCATCA	

Table 2 The antibodies of Western blot assay

Antibodies	Manufacturer	Dilution
MMP-13	Affinity, OH, USA; AF5355	1:2000
ADAMTS-5	Thermo, MA, USA; PA5-32142	1:500
COX-2	Abcam, UK; ab179800	1:1000
Col II	Abcam; ab307674	1:1000
iNOS	Abcam; ab178945	1:1000
Bax	Abcam; ab32503	1:1000
Aggrecan	Affinity; DF7561	1:1000
Bcl-2	Abcam; ab196495	1:1000
Caspase-3	Abcam; ab196495	1:2000
SOX4	Thermo; PA5-72852	2 μg/mL
NLRP3	Affinity; DF7438	1:1000
IL-1β	Affinity; AF5103	1:1000
p20	Affinity; DF15310	1:1000
Drp1	Affinity; DF7037	1:1000
OPA1	Affinity; DF8587	1:1000
Mfn1	Affinity; DF7543	1:1000
Mfn2	Affinity; DF8106	1:2000
Caspase-1	Affinity; AF5418	1:1000
Nrf2	Affinity; AF0639	1:1000
EZH2	Bioss, Beijing, China; bsm-60001R	1:1000
GAPDH	Abcam; ab9485	1:2500
Secondary antibody	Abcam; ab205718	1:2000

adjusted relative to GAPDH. The sequences of the primers are provided in Table 1.

Western blot

Total protein extracts were obtained by lysing NP tissue and cells with RIPA buffer (Thermo). The BCA Kit (Beyotime) was used to measure the protein concentration. Proteins of equal amounts were segregated by sodium dodecyl sulfate-polyacrylamide gel electrophoresis and subsequently transferred onto a polyvinylidene difluoride membrane. The membrane underwent a blocking process with 5% non-fat milk for 1 h and then was incubated with primary antibodies at 4℃ overnight. This was followed by a 1-h incubation with a suitable secondary antibody. Table 2 lists all the antibodies used. Protein bands were visualized on a ChemiDoc Imaging System (Bio-Rad).

Statistical analysis

All data includes at least three replicates and are represented as mean ± standard deviation. One-way analysis of variance was used for comparisons among groups, succeeded by a post hoc Tukey's test. A p-value less than 0.05 was deemed to denote statistical. All statistical evaluations were conducted using GraphPad Prism software version 8.0.

Results

SOX4 expression is upregulated in IDD rats

To investigate the role of SOX4 in IDD, IDD rat model was established. MRI analysis found that IDD group showed lower T2-weighted signal intensity and higher the Pfirrmann grade score in comparison with the control group at 8 weeks post-surgery ($P<0.01$; Fig. S1A). HE staining of NP tissue revealed reduced intervertebral disc cell numbers, disordered arrangement, and abnormal cell morphology in the IDD group compared to the control group (Fig. S1B). Additionally, safranin O staining demonstrated that the content of proteoglycans in the IDD group was significantly reduced compared with the control group (Fig. S1C). Importantly, the mRNA and protein expression of SOX4 in the IDD group was significantly upregulated ($P<0.01$; Fig. S1D–E).

SOX4 knockdown inhibits IDD progression in IDD rats

Subsequently, we constructed an IDD rat model with SOX4 knockdown to further investigate the effect of SOX4 on IDD. qRT-PCR and Western blot analysis showed that SOX4 expression was significantly downregulated in the sh-SOX4 group compared to the sh-NC group ($P<0.01$; Fig. 1A–B). Compared to the sh-NC group, the sh-SOX4 group significantly enhanced the T2-weighted signal and decreased the Pfirrmann grade score at 8 weeks post-surgery ($P<0.01$; Fig. 1C). Furthermore, HE and safranin O staining of NP tissue at week 8

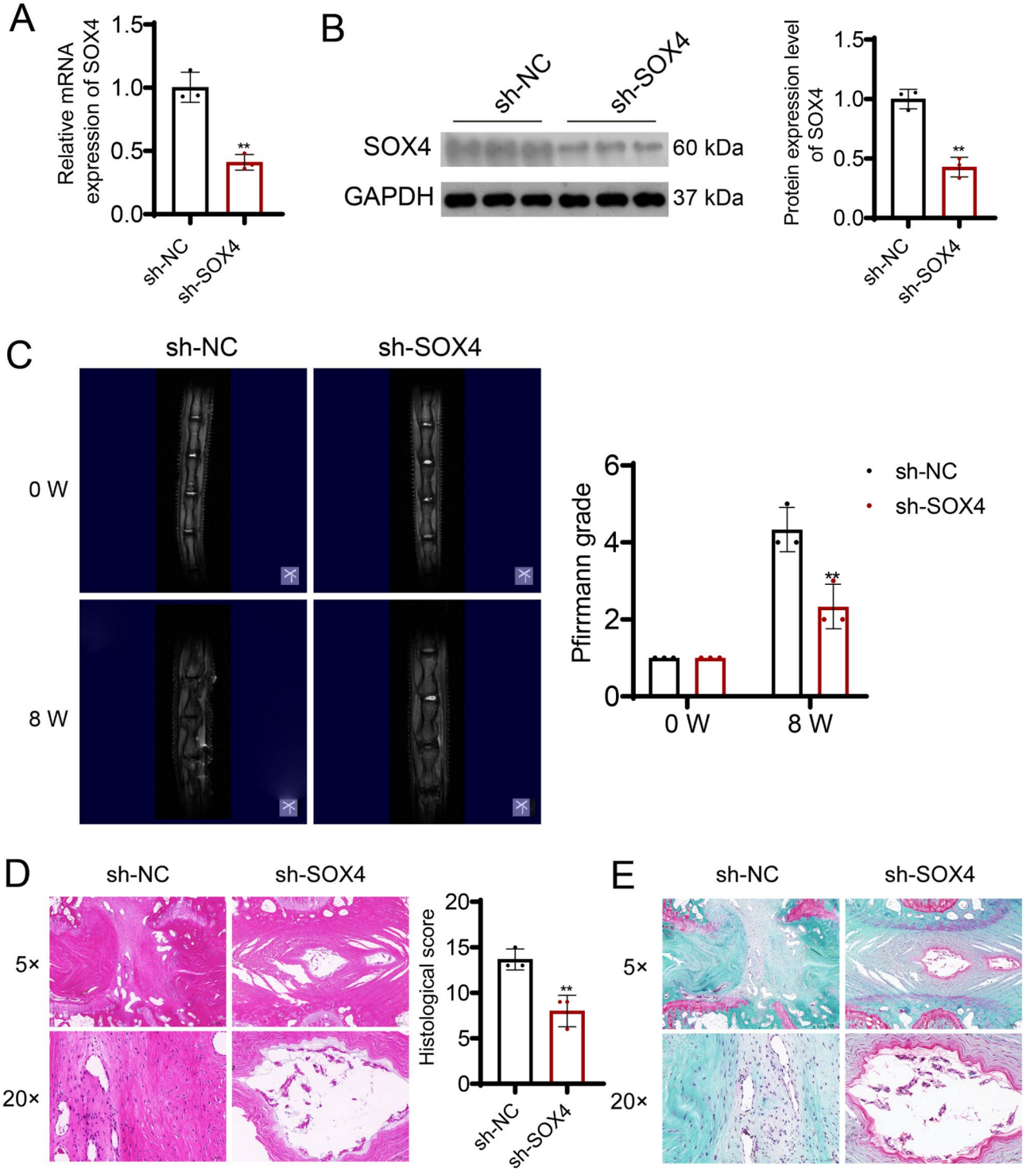

Fig. 1 SOX4 expression is increased in intervertebral disc degeneration (IDD) rats and promotes IDD progression. (**A**–**B**) Quantitative real-time PCR (qRT-PCR) and Western blot analysis showing the expression of SOX4 in the sh-SOX4 and sh-NC groups. (**C**) T2-weighted MRI and Pfirrmann grading at 8 weeks post-surgery for the sh-SOX4 and sh-NC groups. (**D**–**E**) HE staining and safranin O staining of nucleus pulposus (NP) tissue at week 8 post-surgery in the sh-SOX4 and sh-NC groups; magnification: 5× and 20×. $^{**}P < 0.01$ versus the sh-NC group

post-surgery demonstrated that the degenerative changes and disorganization of tissue structure were significantly ameliorated in the sh-SOX4 group compared to the sh-NC group (Fig. 1D–E).

SOX4 knockdown inhibits ECM degradation and NLRP3-mediated pyroptosis in IDD rats

SOX4 have been reported to activate NLRP3 inflammasomes [16, 17] and regulate ECM degradation [20, 21] in IDD progression. Hence, we observed the influence of SOX4 knockdown on ECM degradation and pyroptosis in IDD rats. Firstly, immunohistochemical staining revealed a significant increase in the expression levels of ECM degradation markers (ADAMTS-5 and MMP-13) and the apoptosis marker caspase-3 in the IDD group compared to the control group. In IDD model, the expression levels of ADAMTS-5, MMP-13, and caspase-3 were significantly increased than that in control groups. Whereas, SOX4 knockdown decreased the expression levels of ADAMTS-5, MMP-13, and caspase-3 in IDD rats (Fig. 2A). ECM degradation is associated with the activity of ECM-regulating enzymes, such as matrix metalloproteinases (MMPs) and tissue inhibitors of metalloproteinases (TIMPs) [30]. Therefore, the performance of MMP-1, MMP-2, TIMP-1, and TIMP-2 in IDD model were also investigated using ELISA assay. The results showed upregulated MMP-1 and MMP-2 expression and downregulated TIMP-1 and TIMP-2 expression in IDD model. But SOX4 knockdown reversed their expression patterns, showing as significantly downregulated MMP-1 and MMP-2 and upregulated TIMP-1 and TIMP-2 in sh- SOX4 groups than that in IDD rats ($P < 0.05$; Fig. 2B). Uniformly, SOX4 knockdown notably attenuated the upregulation of pyroptosis markers NLRP3, caspase-1, and IL-1β in IDD rats ($P < 0.05$; Fig. 2C).

SOX4 exacerbates mitochondrial ROS-dependent NLRP3 inflammasome activation in NP cells

To evaluate the effect of SOX4 on IDD in vitro, an IDD cellular model was constructed by stimulating NP cells with IL-1β. The mRNA and protein expression of SOX4 was significantly decreased by sh-SOX4 transfection, whereas it was increased by oe-SOX4 transfection ($P < 0.01$; Fig. 3A–B).

CCK-8 showed that compared with controls, the viability of IL-1β-stimulated NP cells was increased after SOX4 knockdown and decreased after SOX4 overexpression ($P < 0.01$; Fig. 3C). Flow cytometry demonstrated that SOX4 overexpression promoted NP cell apoptosis, whereas SOX4 knockdown inhibited cell apoptosis ($P < 0.01$; Fig. 3D). Meanwhile, transfection with sh-SOX4 resulted in the downregulation of caspase-3 and Bax, and upregulation of Bcl-2 expression in IL-1β-induced NP cells, while oe-SOX4 presented the opposite effects ($P < 0.01$; Fig. 3E). Immunofluorescence analysis revealed that SOX4 knockdown attenuated the expression of NLRP3, GSDMD (pyroptosis marker), and MMP13 (ECM degradation markers) in IL-1β-treated NP cells, while SOX4 overexpression increased their expression (Fig. 4A). Furthermore, TEM was utilized to observe the mitochondrial morphology in NP cells. Results revealed that SOX4 overexpression exacerbated mitochondrial swelling, while its knockdown produced opposite effects (Fig. 4B). Finally, we analyzed NLRP3 inflammasome activation proteins (NLPR3 and p20), ADAMTS-5, and MMP-13 expression using qRT-PCR and Western blotting. The results exhibited that sh-SOX4 administration downregulated the expression of NLRP3, p20, ADAMTS-5, and MMP-13 in IL-1β-induced NP cells (Fig. 4C–D, $P < 0.01$). Conversely, oe-SOX4 transfection upregulated the expression of NLRP3, p20, ADAMTS-5, and MMP-13 ($P < 0.01$; Fig. 4C–D).

To further explore the role of mitochondrial ROS in SOX4-mediated NLRP3 inflammasome activation, NP cells were pre-treated with Mito-tempo (a mitochondrial ROS inhibitor) for 2 h, with or without oe-SOX4/NC transfection. qRT-PCR and Western blotting showed that Mito-tempo had no effect on SOX4 expression (Fig. S2A–B). Whereas, SOX4 overexpression attenuated the reduction of cellular and mitochondrial ROS levels induced by Mito-tempo in NP cells (Fig. 5A-B), indicating that SOX4 can regulate the ROS levels. In addition, Mito-tempo inhibited mitochondrial swelling, an effect that was reversed by the addition of oe-SOX4 (Fig. 5C). Further experiments confirmed that SOX4 overexpression increased levels of 8-OHdG (markers of oxidative stress) in Mito-tempo-treated NP cells ($P < 0.01$; Fig. 5D), indicating a higher oxidative stress level. Moreover, Mito-tempo improved mitochondrial membrane potential, which was reversed by oe-SOX4 (Fig. 6A). Lastly, the downregulation of NLRP3, p20, ADAMTS-5, MMP-13, Drp1, and upregulation of Mfn2 induced by Mito-tempo were reversed upon overexpressing SOX4 (Fig. 6B, $P < 0.01$). However, SOX4 overexpression had no influence on Mito-tempo-induced OPA1 downregulation and Mfn1 upregulation (Fig. 6B). The above evidences indicated that SOX4 enhances mitochondrial ROS-dependent NLRP3 inflammasome activation in NP cells.

SOX4 promotes NLRP3 inflammasome activation in NP cells through upregulating EZH2 expression

Reportedly, EZH2 promotes cartilage endplate degeneration and the progression of IDD [24]. Firstly, we performed ChIP assays to assess the interaction between SOX4 and EZH2. The results indicated a decrease in the enrichment of SOX4 binding to EZH2 fragments following the knockdown of SOX4 ($P < 0.01$; Fig. 7A).

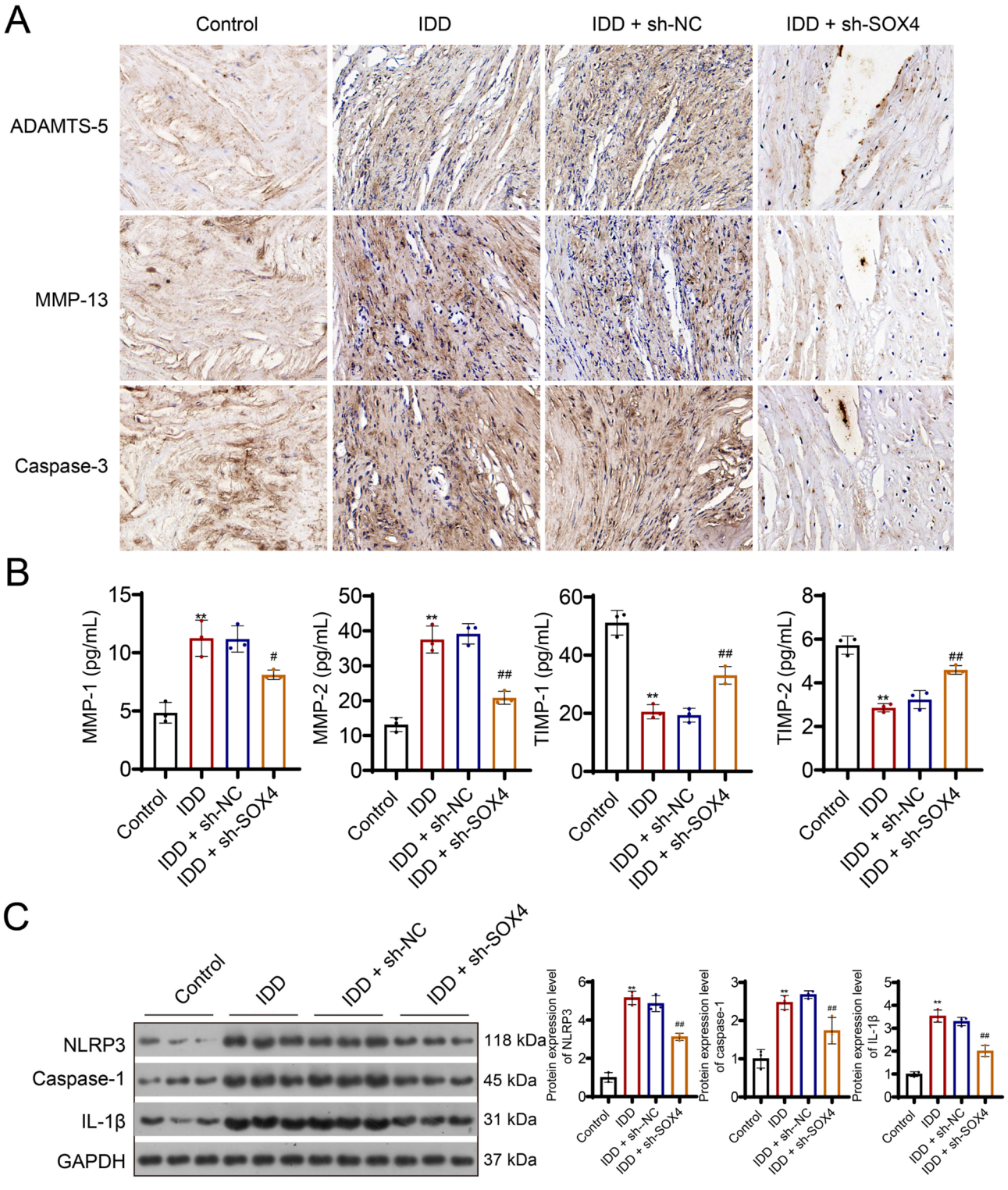

Fig. 2 Knockdown of SOX4 inhibits ECM degradation and NLRP3-mediated pyroptosis in IDD rats. (**A**) Immunohistochemical staining of ADAMTS-5, MMP-13, and caspase-3 in NP tissues from the IDD, control, IDD + sh-SOX4, and IDD + sh-NC groups; scale bar: 20 μm. (**B**) ELISA analysis of the expression of MMP-1, MMP-2, TIMP-1, and TIMP-2 in NP cell supernatants. (**C**) Western blot analysis indicating the protein expression of NLRP3, caspase-1, and IL-1β in NP tissues from the IDD, control, IDD + sh-SOX4, and IDD + sh-NC groups. $^{**}P < 0.01$ versus the control group; $\#P < 0.05$ and $\#\#P < 0.01$ versus the IDD + sh-NC group

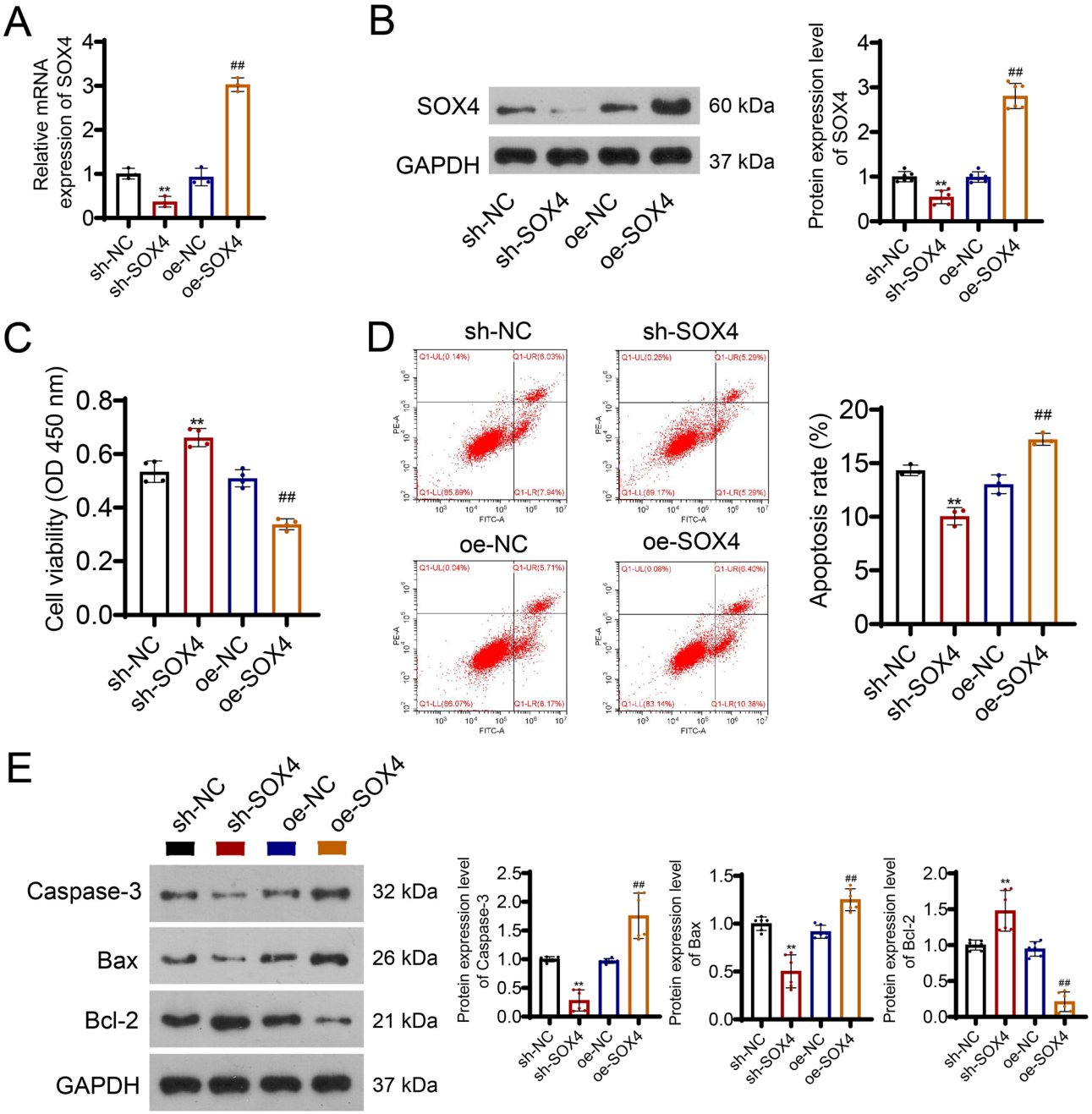

Fig. 3 Evaluation of apoptosis in IL-1β-stimulated NP cells with SOX4 knockdown and overexpression. (**A**-**B**) Detection of SOX4 expression in NP cells using qRT-PCR and Western blotting. (**C**) Cell viability test (CCK-8) showing the effect of SOX4 knockdown and overexpression in IL-1β-stimulated NP cells. (**D**) Flow cytometry analysis of cell apoptosis in IL-1β-stimulated NP cells after knockdown and overexpression of SOX4. (**E**) Western blot analysis of apoptosis markers (caspase-3, Bcl-2, and Bax) in IL-1β-induced NP cells after sh-SOX4 and oe-SOX4 transfection. $^{**}P < 0.01$ versus the sh-NC group; $\#\#P < 0.01$ versus the oe-NC group

Immunofluorescence analysis demonstrated that SOX4 and EZH2 co-localized in the nucleus of NP cells (Fig. 7B).

To examine the influence of EZH2 on mitochondrial ROS and inflammasome activation, IL-1β-induced NP cells were treated with sh-SOX4, with or without oe-EZH2. qRT-PCR and Western blot results showed that oe-EZH2 significantly increased EZH2 expression but had no effect on SOX4 expression (Fig. 7C–D, $P < 0.01$). Meanwhile, SOX4 knockdown reversed oe-EZH2-induced EZH2 upregulation ($P < 0.01$; Fig. 7C–D). These results indicated that EZH2 is a regulatory factor of SOX4. Subsequently, MitoSOX Red staining revealed that oe-EZH2-induced increase in ROS production in

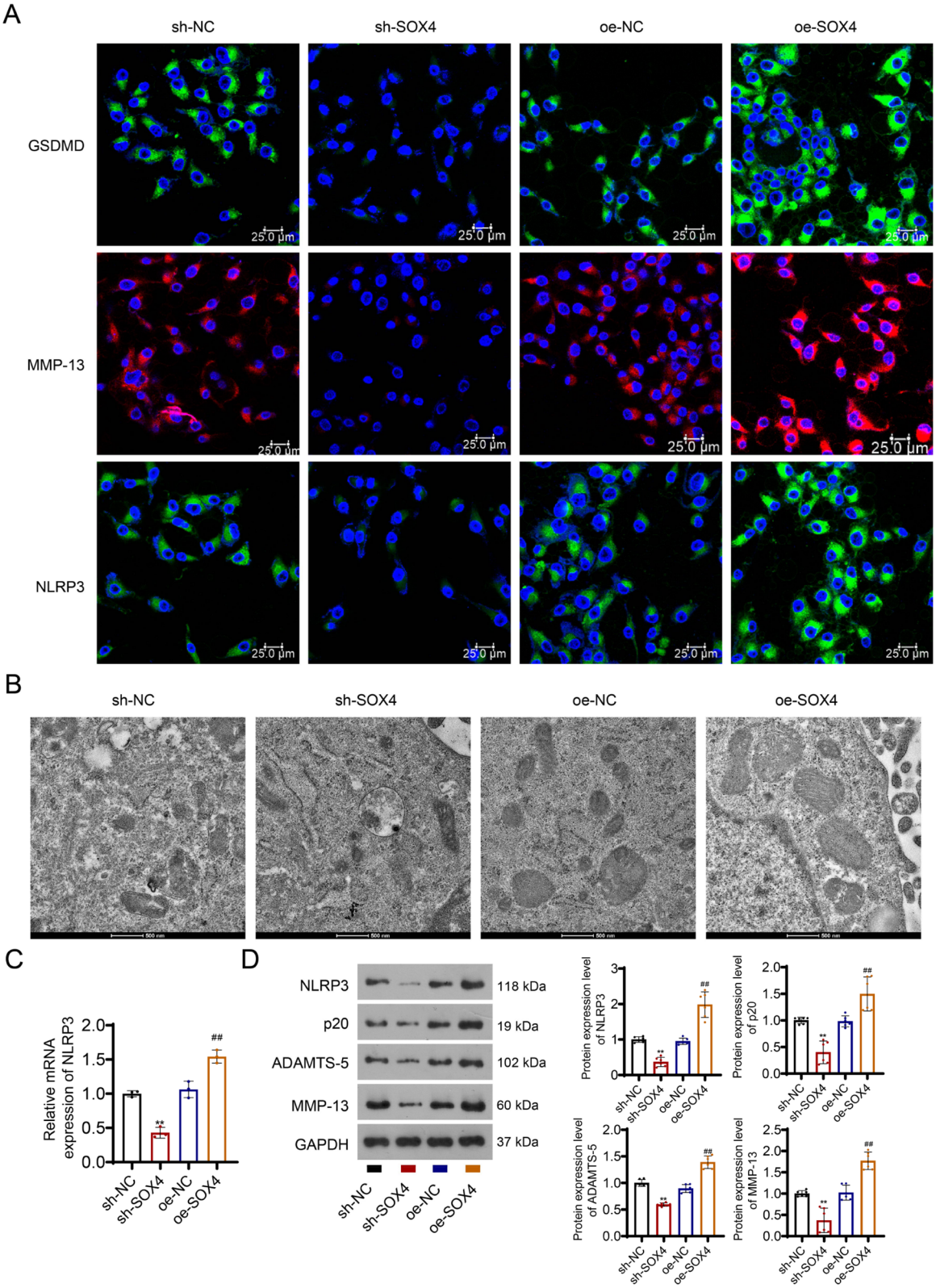

Fig. 4 SOX4 exacerbates NLRP3 inflammasome activation in NP cells. (**A**) Immunofluorescence analysis to assess the expression of GSDMD (pyroptosis marker), MMP13, and NLRP3 in IL-1β-treated NP cells with SOX4 knockdown and overexpression; scale bar: 25 μm. (**B**) Transmission Electron Microscopy (TEM) images showing the mitochondrial morphology in NP cells with SOX4 knockdown and overexpression; scale bar: 500 nm. (**C**–**D**) qRT-PCR or Western blot analysis of NLRP3 inflammasome activation proteins (NLPR3 and p20), ADAMTS-5, and MMP-13 in IL-1β-induced NP cells with SOX4 knockdown and overexpression. $^{**}P < 0.01$ versus the sh-NC group; $^{\#\#}P < 0.01$ versus the oe-NC group

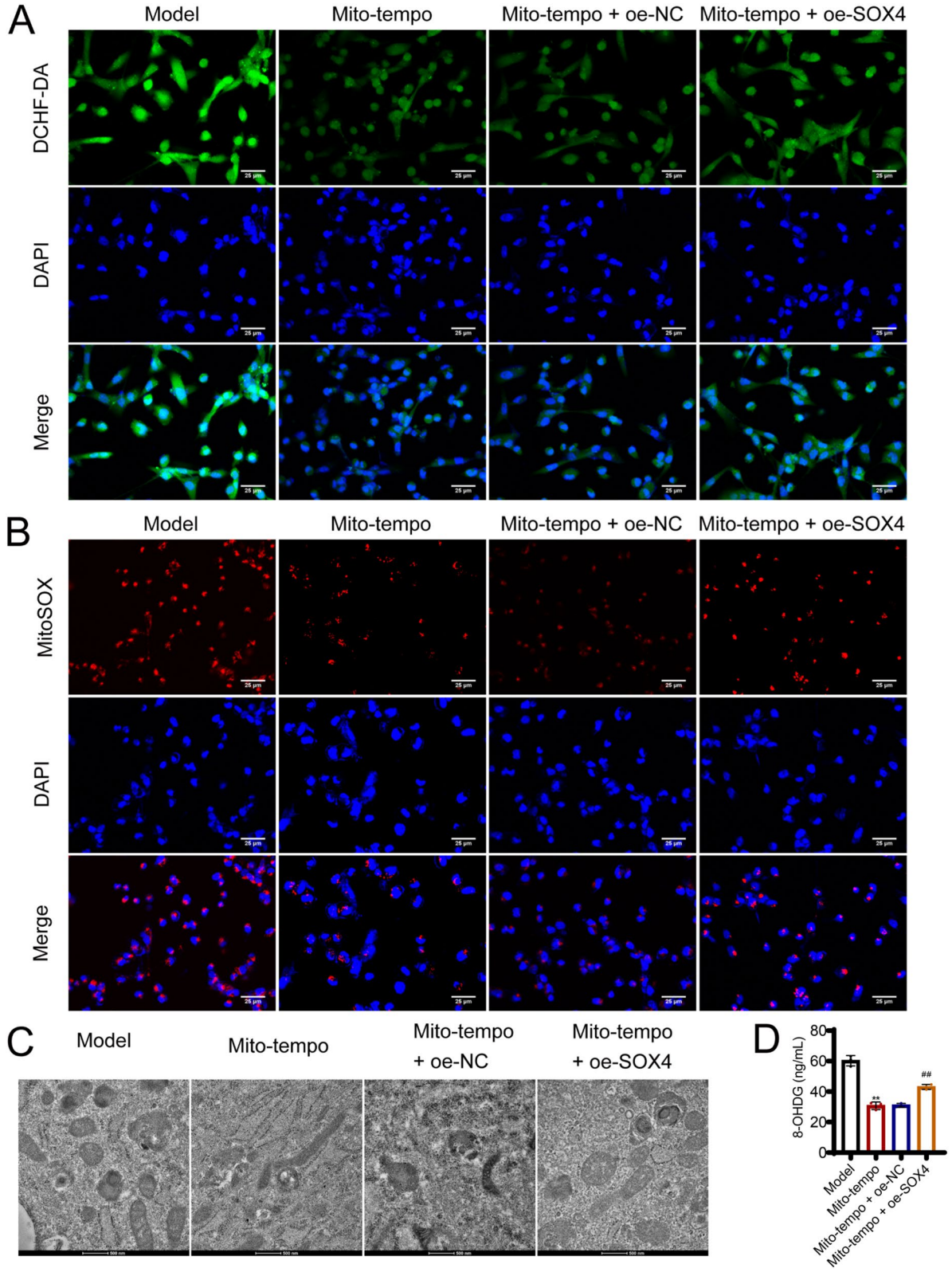

Fig. 5 SOX4 overexpression induces the mitochondrial damage in NP cells. (**A**) The H_2DCF-DA assay analyzed the intracellular ROS levels of NP cells following Mito-tempo treatment and/or SOX4 overexpression; scale bar: 25 μm. (**B**) MitoSOX Red staining demonstrating mitochondrial ROS levels in NP cells; scale bar: 25 μm. (**C**) TEM images displaying mitochondrial morphology in NP cells; scale bar: 100 nm. (**D**) Levels of 8-OHdG in NP cells were measured by ELISA. $^{**}P < 0.01$ versus the model group; $\#\#P < 0.01$ versus the Mito-tempo + oe-NC group

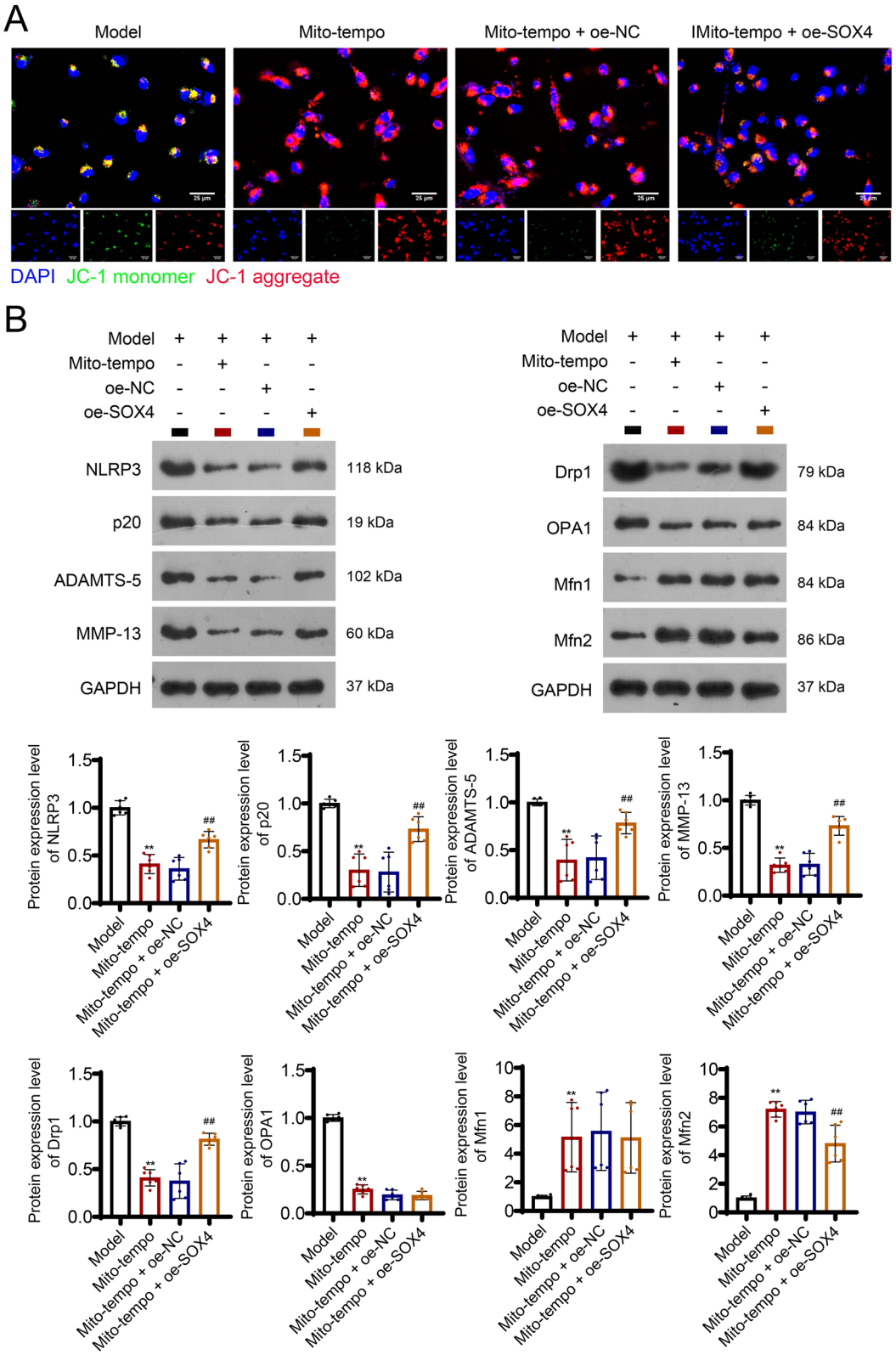

Fig. 6 SOX4 overexpression induces the mitochondrial damage in NP cells by promoting NLRP3 inflammasome activation. (**A**) JC-1 assay results displaying the mitochondrial membrane potential in NP cells pre-treated with Mito-tempo and/or oe-SOX4/NC transfection; scale bar: 25 μm. (**B**) Western blot analysis indicating the protein expression of NLPR3, p20, ADAMTS-5, MMP-13, and mitochondrial morphology-related proteins (Drp1, OPA1, Mfn1/2) following Mito-tempo treatment and/or SOX4 overexpression. $^{**}P < 0.01$ versus the model group; $\#\#P < 0.01$ versus the Mito-tempo + oe-NC group

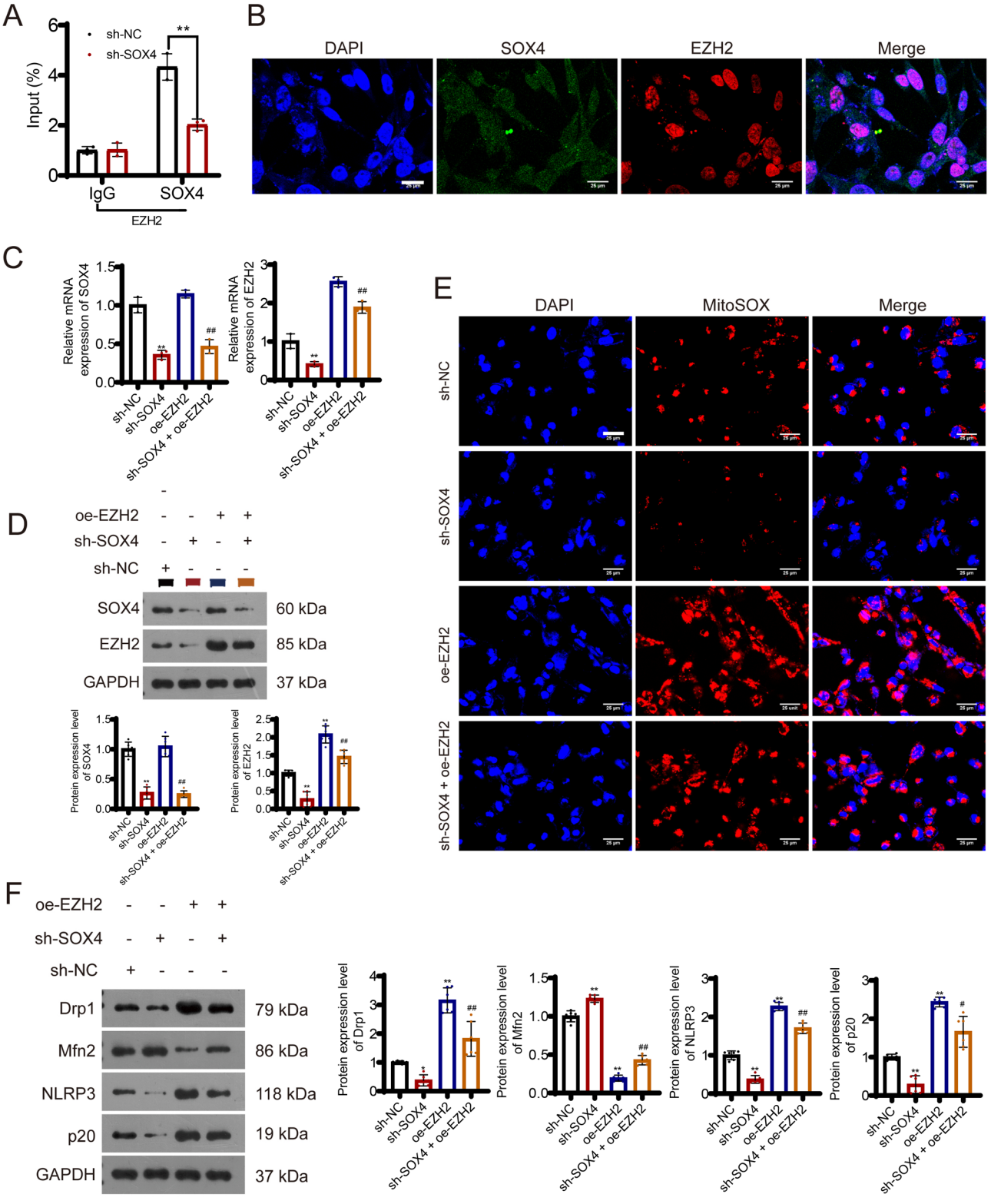

Fig. 7 SOX4 promotes NLRP3 inflammasome activation in NP cells through upregulating EZH2 expression. (**A**) NP cells were infected with indicated sh-NC or sh-SOX4. Cells were collected for ChIP-qRT-PCR analysis using the IgG or SOX4 antibody in NP cells. (**B**) Immunofluorescence analysis displaying co-localization of SOX4 and EZH2 in the nucleus of NP cells; scale bar: 25 μm. (**C**–**D**) qRT-PCR and Western blot analysis demonstrating the expression of SOX4 and EZH2 after oe-EZH2 and/or sh-SOX4 transfection in IL-1β-induced NP cells. (**E**) MitoSOX Red staining showing mitochondrial ROS production in NP cells after oe-EZH2 and/or sh-SOX4 transfection; scale bar: 25 μm. (**F**) Western blot analysis indicating the protein expression of NLRP3, p20, Drp1, and Mfn2 following oe-EZH2 and/or sh-SOX4 transfection. *$P < 0.05$ and **$P < 0.01$ versus the sh-NC group; #$P < 0.05$ and ##$P < 0.01$ versus the oe-EZH2 group

mitochondria was attenuated after sh-SOX4 transfection (Fig. 7E). Lastly, Lastly, Western blotting indicated that oe-EZH2-induced the upregulation of NLRP3, p20, and Drp1 and Mfn2 downregulation was reversed by transfecting sh-SOX4 ($P < 0.05$; Fig. 7F).

SOX4 promotes NLRP3 inflammasome activation in NP cells by modulating the EZH2/NRF2 pathway

Reportedly, the EZH2/NRF2 pathway has been related to mitochondrial dysfunction [31]; therefore, we pretreated NP cells with the Nrf2 inhibitor ML385 (1 μM) for 1 h prior to sh-SOX4 treatment. As shown in Fig. 8A–B, ML385 suppressed Nrf2 expression ($P < 0.01$) and had no effect on SOX4 and EZH2 expression. SOX4 knockdown decreased SOX4 and EZH2 expression and weakened ML385-induced Nrf2 downregulation ($P < 0.05$; Fig. 8A-B). In addition, treatment with ML385 decreased NP cell viability, which was reversed upon the addition of sh-SOX4 ($P < 0.01$; Fig. 8C). Levels of 8-OHdG in NP cells were found to be increased by ML385 treatment and significantly decreased by sh-SOX4 addition ($P < 0.01$; Fig. 8D). Moreover, treatment with ML385 induced a decrease in mitochondrial membrane potential and an increase in ROS levels ($P < 0.01$). This effect was reversed upon the addition of sh-SOX4 ($P < 0.05$; Fig. 8E–F). Finally, Western blotting revealed that the ML385-induced upregulation of NLRP3, p20, OPA1, and Drp1, along with the downregulation of Mfn1 and Mfn2, was reversed by the addition of sh-SOX4 ($P < 0.01$; Fig. 8G).

SOX4 promotes NLRP3 activation by modulating the EZH2/Nrf2 pathway, thereby inducing pyroptosis in NP cells and accelerating ECM degradation

To further confirm whether SOX4 promotes NLRP3 activation through modulation of the EZH2/Nrf2 pathway, subsequently promoting pyroptosis and ECM degradation in NP cells, we pretreated NP cells with the Nrf2 agonist sulforaphane (5 μM) for 1 h. As shown in Fig. S3A–B, qPCR and Western blot results indicated that sulforaphane treatment increased Nrf2 expression ($P < 0.01$), while it had no effect on SOX4 and EZH2 expression. Next, CCK-8 assay ascertained that the detrimental effects of EZH2 overexpression on cell viability were reversed by the administration of sulforaphane ($P < 0.01$; Fig. S3C). Immunofluorescence staining revealed that the downregulation of NLRP3, GSDMD, and MMP13 induced by overexpressed EZH2 was reversed upon the addition of sulforaphane (Fig. S3D). Western blotting demonstrated that the increased effects of overexpressed EZH2 on NLRP3, caspases-1, and IL-1β, as well as the adverse effects on Aggrecan and Col II, were reversed by the addition of sulforaphane ($P < 0.05$; Fig. S3E). Finally, ELISA results showed that sulforaphane administration attenuated oe-EZH2-induced MMP-1 and MMP-2 upregulation and TIMP-1 and TIMP-2 downregulation ($P < 0.05$; Fig. S3F).

Discussion

IDD is a prevalent degenerative condition in clinical practice [32]; however, many aspects of the underlying mechanisms remain poorly understood. Earlier findings highlight NP cell dysfunction and NP tissue damage as crucial aspects of IDD [33]. Numerous studies have explored maintaining NP cell homeostasis as a potential treatment for IDD [34]. In addition, inflammation can alter the NP cell microenvironment, leading to apoptosis or pyroptosis, ultimately contributing to IDD [35]. In the present study, IDD rat and cell models were established, and SOX4 deficiency was found to ameliorate ROS-dependent NLRP3 inflammasome activation and ECM degradation by inhibiting EZH2/NRF2 pathways, and thus ameliorate the impairment of NP cell and tissue homeostasis.

SOX4, a member of the SOX (SRY-related HMG box) gene family, is highly conserved in vertebrates and encodes a 47 KD protein containing 474 amino acid residues [36, 37]. Recently, SOX4 is reported to play pivotal roles in the development of bone, islet and heart, and cancers [14, 38, 39]. Previous studies have suggested that SOX4 is highly expressed in most of the cancers and promotes tumor progression [36, 40, 41]. In IDD, SOX4 has also been demonstrated to be highly expressed and is associated with IDD progression [20, 21]. And a recent study emphasizes that SOX4 is an effective therapy targets for IDD, which showed that inhibition of SOX4 can delay disc degeneration and lower back pain [42]. Our results showed similar outcomes with these previous reported results, and also demonstrated the inhibitory role of absent SOX4 in IDD, showing as that SOX4 deficiency ameliorates NP tissue disorganization and ECM degradation.

ECM degradation, causing loss of structural integrity and function, is a well-documented feature of IDD [34, 43]. Maintaining the balance between ECM synthesis and degradation is vital for NP tissue homeostasis. Disruption in this balance, particularly via upregulated MMPs and ADAMTSs, may contribute to IDD development [44]. Our study demonstrated that the knockdown of SOX4 hindered ECM degradation in NP cells by downregulating catabolic markers (ADAMTS-5 and MMP-13) and upregulating anabolic markers (Col II and Aggrecan). These results indicate that SOX4 plays a role in modulating ECM degradation in IDD rats, thereby contributing to IDD progression.

Moreover, the dysfunction of various organelles, especially mitochondria, is closely related to denaturation [45]. Mitochondrial dysfunction and ROS production in NP cells are key factors contributing to IDD [43]. In our

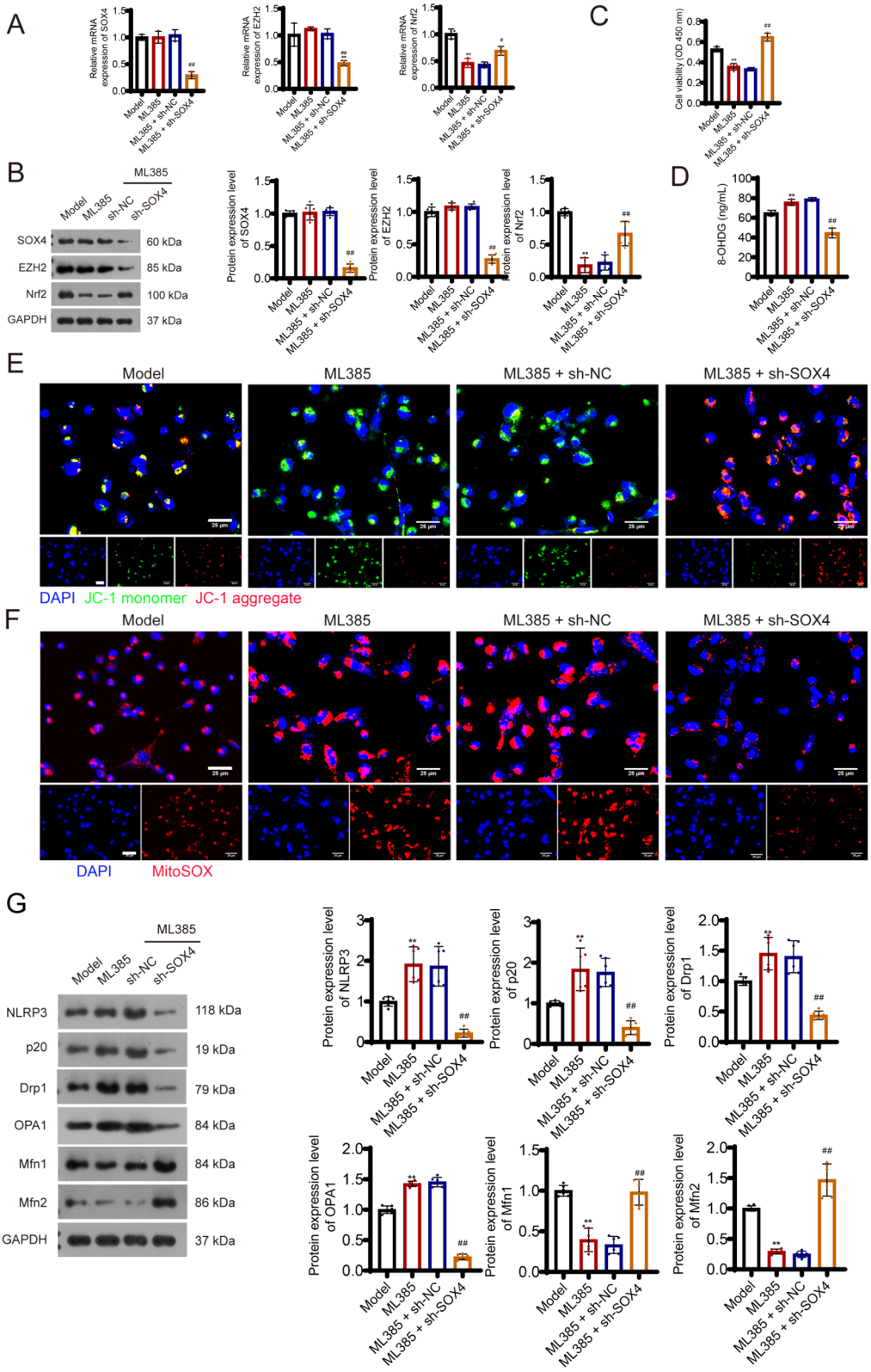

Fig. 8 (See legend on next page.)

(See figure on previous page.)

Fig. 8 SOX4 enhances NLRP3 inflammasome activation in NP cells via the EZH2/Nrf2 pathway. (**A**–**B**) qRT-PCR and Western blot analysis showing the expression of SOX4, EZH2, and Nrf2 in NP cells after treatment with ML385 and/or sh-SOX4. (**C**) CCK8 assay results demonstrating cell viability after treatment with ML385 and/or sh-SOX4. (**D**) Levels of 8-OHdG in NP cells were measured by ELISA. (**E**) JC-1 assay indicating the mitochondrial membrane potential after treatment with ML385 and/or sh-SOX4; scale bar: 25 μm. (**F**) DCFH-DA probe showing ROS levels in NP cells after treatment with ML385 and/or sh-SOX4; scale bar: 25 μm. (**G**) Western blot analysis of NLPR3, p20, Drp1, OPA1, Mfn1, and Mfn2 protein expression in NP cells following treatment with ML385 and/or sh-SOX4. *$P < 0.05$ and **$P < 0.01$ versus the Model group; #$P < 0.05$ and ##$P < 0.01$ versus the ML385 + sh-SOX4 group

study, overexpressed SOX4 exacerbated mitochondrial swelling in IL-1β-induced NP cells, while knockdown produced opposite effects. Furthermore, interference with SOX4 expression resulted in a decrease in intracellular and mitochondrial ROS levels in IL-1β-induced NP cells. Overexpression of SOX4 attenuated the reduction in mitochondrial ROS levels induced by Mito-tempo (a mitochondrial ROS inhibitor). These results indicated that SOX4 promotes IDD progression through inducing dysfunction of mitochondria.

NLRP3 inflammasome is a key effector molecule of cell death due to its intricate transcriptional and post-translational modifications [46]. Mitochondria is also reported to contribute to the activation of the NLRP3 inflammasome via mitochondrial dysfunction and the generation of ROS [47], and thus affecting NP cell metabolism and inducing pyroptosis [48]. Moreover, pyroptosis is involved in IDD pathogenesis and contribute to NP cell death and ECM degradation [49, 50]. The We observed that suppressing SOX4 expression inhibited pyroptosis in NP cells by reducing NLRP3, caspase-1, and IL-1β levels. This highlights the role of SOX4 in regulating NLRP3 inflammasome activation and pyroptosis in the progression of IDD. Concurrently, overexpression of SOX4 reversed the Mito-tempo-induced downregulation of NLRP3, p20, Drp1, ADAMTS-5, and MMP-13, while also inhibiting the Mfn2 upregulation. Our results suggest that inhibition of SOX4 expression could hinder mitochondrial ROS-dependent NLRP3 inflammasome activation, thereby mitigating the progression of IDD.

Although the role of SOX4 in IDD have been investigated in several studies [20, 21, 42], the underline mechanism is still insufficiency. A previous study revealed that knocking down EZH2 protects against cartilage endplate and disc degeneration, easing symptoms and slowing IDD progression [24]. EZH2, a histone methyltransferase,

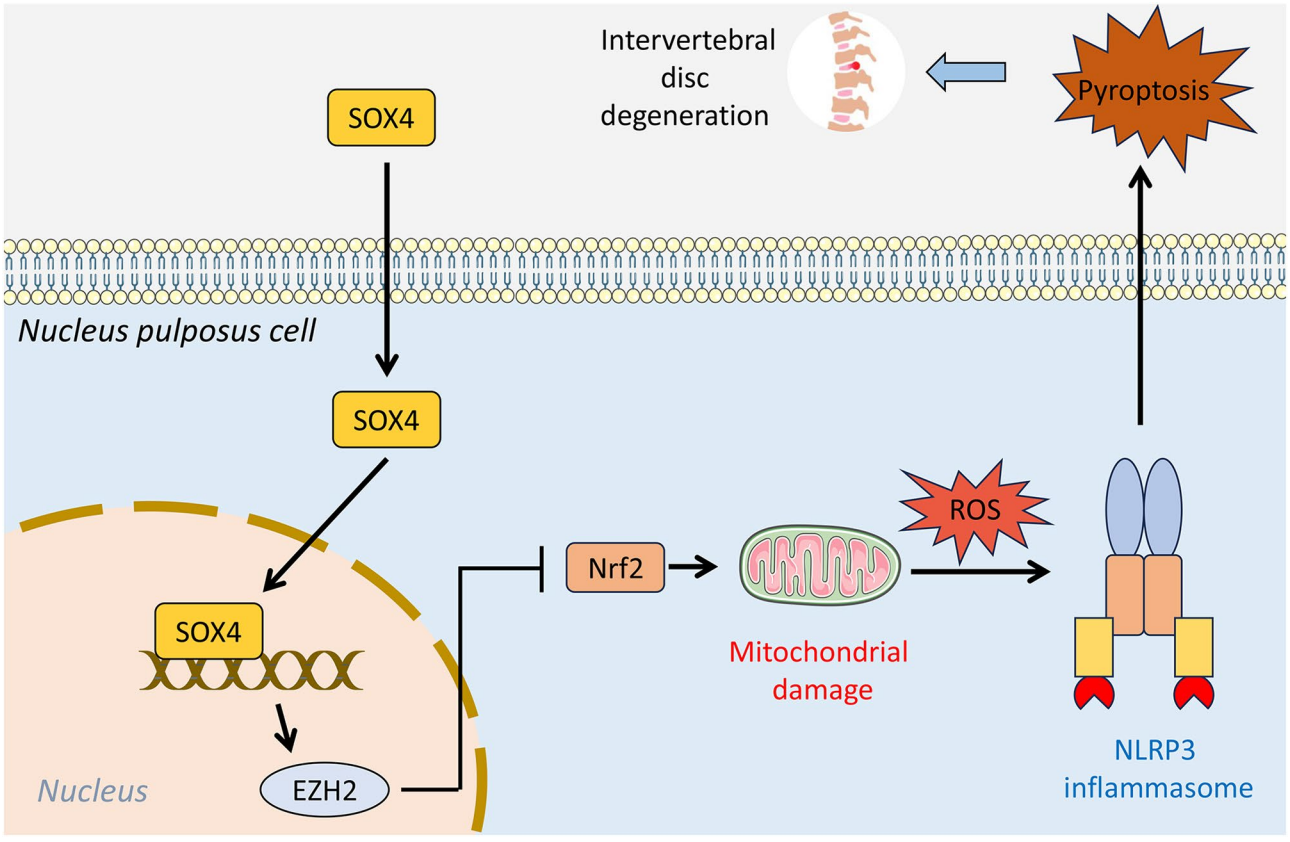

Fig. 9 A schematic diagram illustrating the mechanism of SOX4 in intervertebral disc degeneration

has been documented to participate in the regulation of numerous cellular activities, such as cell proliferation, differentiation, and programmed cell death [51]. EZH2 can suppress Nrf2 expression, thereby inducing inflammasome activation and ROS production [26]. Furthermore, recent studies reported that SOX4 can directly regulate EZH2 in various diseases [22, 23, 52], but their regulatory effects of them remains unknown in IDD. Here, we hypothesized that SOX4 may modulate the NRF2 pathway through EZH2, in response to mitochondrial ROS-dependent activation of NLRP3 inflammasomes in NP cells, promoting IDD progression. In our results, SOX4 and EZH2 co-localized in the nucleus of NP cells was observed. Meanwhile, SOX4 knockdown reversed the increase in mitochondrial ROS levels and the expression of NLRP3, p20, and Drp1 caused by EZH2 overexpression in NP cells. It also countered the reduction of Mfn2 induced by EZH2 overexpression in NP cells. We additionally observed that inhibiting SOX4 enhanced the expression of NRF2, an effect offset by an elevation in EZH2. Furthermore, the heightened ROS production and NLRP3 inflammasome activation induced by EZH2 overexpression were mitigated upon SOX4 knockdown. These findings suggest a regulatory role of SOX4 in the EZH2/NRF2 pathway. Moreover, after SOX4 knockdown, ML385 (NRF2 inhibitor)-induced ROS increase and NLRP3 inflammasome activation were reversed. Additionally, NRF2 activator sulforaphane administration mitigated the positive effects of EZH2 overexpression on IDD progression, including reduced ROS production, NLRP3 inflammasome activation, NP cell pyroptosis, and ECM degradation.

In this study, we found that the knockdown of SOX4 can alleviate IDD progression by suppressing NLRP3 inflammasome activation via the regulation of the EZH2/Nrf2 pathway (Fig. 9). While our study yields robust findings, it is essential to acknowledge certain limitations. Firstly, a significant portion of our experiments was conducted in vitro or in animal models. To enhance the applicability and relevance of our findings to clinical practice, further confirmation in human subjects with IDD is warranted. Secondly, our focus was primarily on the EZH2/Nrf2 pathway, and exploration of other molecular pathways implicated in SOX4-mediated IDD progression remains an avenue for future investigation. Despite these limitations, our research significantly contributes to elucidating the molecular mechanisms involved in IDD progression and identifying potential therapeutic targets.

Conclusion

Our findings underscore that SOX4 suppresses mitochondrial ROS-dependent NLRP3 inflammasome activation and ECM degradation via modulating the EZH2/Nrf2 pathway, thereby ameliorating the impairments of NP cells and inhibiting IDD progression. Our study might shed light on the acknowledge of mechanism involved in IDD progression and indicated that SOX4 might be a therapeutic target for IDD degeneration.

Abbreviations

IDD	Intervertebral disc degeneration
NP	Nucleus pulposus
ECM	Extracellular matrix
ROS	Reactive oxygen species
SOX4	SRY-related HMG-box 4
NC	Negative control
NP	Nucleus pulposus
MRI	Magnetic resonance imaging
HE	Hematoxylin and eosin
TEM	Transmission electron microscopy
qRT-PCR	Quantitative real-time PCR
MMPs	Matrix metalloproteinases
TIMPs	Tissue inhibitors of metalloproteinases

Supplementary Information

The online version contains supplementary material available at https://doi.org/10.1186/s12967-024-05913-1.

Supplementary Material 1

Acknowledgements

We thank Yangzhou University for providing equipment, premises and ethical supervision for animal experiment.

Author contributions

Wenzhi Zhao: Conceptualization, Data curation, Formal analysis, Investigation, and Writing-original draft. Guiqi Zhang: Conceptualization, Data curation, Methodology, Software, Visualization, Funding acquisition and Writing-review & editing. Yadong Liu: Data curation, Formal analysis, Funding acquisition and Validation. Yunxiang Hu: Data curation, Formal analysis, Funding acquisition and Validation. Milad Ashrafizadeh, Writing-reviewing paper, revising and improving its quality. All authors have read and approved the final manuscript.

Funding

This work was supported by ["Provincial Key Specialties" Independent Scientific Research Project of Dalian Municipal Central Hospital] (Grant number [2023SZ028]), [Doctoral Scientific Research Foundation of Liaoning Province] (Grant number [2020-BS-280]) and [the Natural Science Foundation of Dalian] (Grant numbers [21Z11019] and [2021RQ025].

Data availability

The datasets used and/or analysed during the current study are available from the corresponding author on reasonable request.

Declarations

Ethics approval and consent to participate

This study was performed in line with the principles of the Declaration of Helsinki. Approval was granted by the Ethics Committee of Yangzhou University (No. 202306014).

Consent for publication

Not applicable.

Conflict of interest

The authors declare no conflict of interest.

Author details
[1]Department of Traumatic Orthopedics, The Second Affiliated Hospital, Dalian Medical University, Dalian 116011, China
[2]Department of Spinal Surgery, Dalian Municipal Central Hospital, Dalian 116033, China

Received: 13 November 2023 / Accepted: 22 November 2024
Published online: 03 April 2025

References

1. Zhang GZ, et al. NF-κB signalling pathways in nucleus pulposus cell function and intervertebral disc degeneration. Cell Prolif. 2021;54(7):e13057.
2. Wang J, et al. The Regulatory Effect of MicroRNA-101-3p on Disc Degeneration by the STC1/VEGF/MAPK pathway. Oxid Med Cell Longev. 2021;2021:p1073458.
3. Gao S, et al. A potential target gene CD63 for different degrees of intervertebral disc degeneration. Sci Rep. 2022;12(1):957.
4. Liao C-R, et al. Advanced oxidation protein products increase TNF-α and IL-1β expression in chondrocytes via NADPH oxidase 4 and accelerate cartilage degeneration in osteoarthritis progression. Redox Biol. 2020;28:101306–101306.
5. Guo HY, et al. Emerging evidence on noncoding-RNA regulatory machinery in intervertebral disc degeneration: a narrative review. Arthritis Res Ther. 2020;22(1):270.
6. Desmoulin GT, Pradhan V, Milner TE. Mechanical aspects of intervertebral disc Injury and implications on Biomechanics. Spine (Phila Pa 1976). 2020;45(8):E457–64.
7. Kang L, et al. The mitochondria-targeted anti-oxidant MitoQ protects against intervertebral disc degeneration by ameliorating mitochondrial dysfunction and redox imbalance. Cell Prolif. 2020;53(3):e12779.
8. Tschoeke SK, et al. Apoptosis of human intervertebral discs after trauma compares to degenerated discs involving both receptor-mediated and mitochondrial-dependent pathways. J Orthop Res. 2008;26(7):999–1006.
9. Liu Q, et al. The role of mitochondria in NLRP3 inflammasome activation. Mol Immunol. 2018;103:115–24.
10. Xia C, et al. Mesenchymal stem cell-derived exosomes ameliorate intervertebral disc degeneration via anti-oxidant and anti-inflammatory effects. Free Radic Biol Med. 2019;143:1–15.
11. Luo J et al. Role of Pyroptosis in intervertebral disc degeneration and its therapeutic implications. Biomolecules, 2022. 12(12).
12. Xing H, et al. Injectable exosome-functionalized extracellular matrix hydrogel for metabolism balance and pyroptosis regulation in intervertebral disc degeneration. J Nanobiotechnol. 2021;19(1):264.
13. Mariotte A, et al. A mouse model of MSU-induced acute inflammation in vivo suggests imiquimod-dependent targeting of Il-1β as relevant therapy for gout patients. Theranostics. 2020;10(5):2158–71.
14. Moreno CS. SOX4: the unappreciated oncogene. Semin Cancer Biol. 2020;67(Pt 1):57–64.
15. Grimm D, et al. The role of SOX family members in solid tumours and metastasis. Semin Cancer Biol. 2020;67(Pt 1):122–53.
16. Wei H, Gu Q. SOX4 promotes high-glucose-induced inflammation and angiogenesis of retinal endothelial cells by activating NF-κB signaling pathway. Open Life Sci. 2022;17(1):393–400.
17. Xiao L, et al. Interleukin-6 mediated inflammasome activation promotes oral squamous cell carcinoma progression via JAK2/STAT3/Sox4/NLRP3 signaling pathway. J Exp Clin Cancer Res. 2022;41(1):166.
18. Wang H, et al. Human bone marrow mesenchymal stromal cell-derived extracellular vesicles promote proliferation of degenerated Nucleus Pulposus cells and the synthesis of Extracellular Matrix through the SOX4/Wnt/β-Catenin Axis. Front Physiol. 2021;12:723220.
19. Hu B, et al. MECHANISM OF MIR-25-3P CARRIED BY EXTRACELLULAR VESICLES DERIVED FROM PLATELET-RICH PLASMA IN IL-1β-INDUCED NUCLEUS PULPOSUS CELL DEGENERATION VIA THE SOX4/CXCR7 AXIS. Shock. 2022;58(1):56–67.
20. Sun JC, et al. MiR-499a-5p suppresses apoptosis of human nucleus pulposus cells and degradation of their extracellular matrix by targeting SOX4. Biomed Pharmacother. 2019;113:108652.
21. Zhang F, et al. Circular RNA ITCH promotes extracellular matrix degradation via activating Wnt/β-catenin signaling in intervertebral disc degeneration. Aging. 2021;13(10):14185–97.
22. Yan X, et al. The SOX4/EZH2/SLC7A11 signaling axis mediates ferroptosis in calcium oxalate crystal deposition-induced kidney injury. J Transl Med. 2024;22(1):9.
23. Li L, et al. A TGF-β-MTA1-SOX4-EZH2 signaling axis drives epithelial-mesenchymal transition in tumor metastasis. Oncogene. 2020;39(10):2125–39.
24. Jiang C, et al. Inhibition of EZH2 ameliorates cartilage endplate degeneration and attenuates the progression of intervertebral disc degeneration via demethylation of Sox-9. EBioMedicine. 2019;48:619–29.
25. Zhou M, et al. EZH2 upregulates the expression of MAPK1 to promote intervertebral disc degeneration via suppression of miR-129-5. J Gene Med. 2022;24(3):e3395.
26. Cai LJ, et al. LncRNA MALAT1 facilitates inflammasome activation via epigenetic suppression of Nrf2 in Parkinson's disease. Mol Brain. 2020;13(1):130.
27. Luo X, et al. Ulinastatin ameliorates IL-1β-Induced Cell Dysfunction in Human Nucleus Pulposus cells via Nrf2/NF-κB pathway. Oxid Med Cell Longev. 2021;2021:p5558687.
28. Chen Y, et al. Melatonin ameliorates intervertebral disc degeneration via the potential mechanisms of mitophagy induction and apoptosis inhibition. J Cell Mol Med. 2019;23(3):2136–48.
29. Chen Y, et al. Mfn2 is involved in intervertebral disc degeneration through autophagy modulation. Osteoarthritis Cartilage. 2020;28(3):363–74.
30. Kwon WK, et al. The role of Hypoxia in Angiogenesis and Extracellular Matrix Regulation of intervertebral disc cells during inflammatory reactions. Neurosurgery. 2017;81(5):867–75.
31. Li J, et al. Ginsenoside Rg1 reduced Microglial activation and mitochondrial dysfunction to Alleviate Depression-Like Behaviour Via the GAS5/EZH2/SOCS3/NRF2 Axis. Mol Neurobiol. 2022;59(5):2855–73.
32. Kos N, Gradisnik L, Velnar T. A brief review of the degenerative intervertebral disc disease. Med Arch. 2019;73(6):421–4.
33. Johnson ZI, Shapiro IM, Risbud MV. Extracellular osmolarity regulates matrix homeostasis in the intervertebral disc and articular cartilage: evolving role of TonEBP. Matrix Biol. 2014;40:10–6.
34. Alvarez-Garcia O, et al. FOXO are required for intervertebral disk homeostasis during aging and their deficiency promotes disk degeneration. Aging Cell. 2018;17(5):e12800.
35. Lyu FJ, et al. Painful intervertebral disc degeneration and inflammation: from laboratory evidence to clinical interventions. Bone Res. 2021;9(1):7.
36. Vervoort SJ, van Boxtel R, Coffer PJ. The role of SRY-related HMG box transcription factor 4 (SOX4) in tumorigenesis and metastasis: friend or foe? Oncogene. 2013;32(29):3397–409.
37. She ZY, Yang WX. SOX family transcription factors involved in diverse cellular events during development. Eur J Cell Biol. 2015;94(12):547–63.
38. Cheng CK, et al. SOX4 is a novel phenotypic regulator of endothelial cells in atherosclerosis revealed by single-cell analysis. J Adv Res. 2023;43:187–203.
39. Kuo CY, et al. SOX4 is a pivotal regulator of tumorigenesis in differentiated thyroid cancer. Mol Cell Endocrinol. 2023;578:112062.
40. Ma H, et al. The Sox4/Tcf7l1 axis promotes progression of BCR-ABL-positive acute lymphoblastic leukemia. Haematologica. 2014;99(10):1591–8.
41. Zhang J, et al. SOX4 promotes the growth and metastasis of breast cancer. Cancer Cell Int. 2020;20:468.
42. Huang Y, et al. Acetylshikonin promoting PI3K/Akt pathway and inhibiting SOX4 expression to delay intervertebral disc degeneration and low back pain. J Orthop Res. 2024;42(1):172–82.
43. Tan Y, et al. Bone morphogenetic protein 2 alleviated intervertebral disc degeneration through mediating the degradation of ECM and apoptosis of nucleus pulposus cells via the PI3K/Akt pathway. Int J Mol Med. 2019;43(1):583–92.
44. Zhao Y, et al. Cortistatin protects against intervertebral disc degeneration through targeting mitochondrial ROS-dependent NLRP3 inflammasome activation. Theranostics. 2020;10(15):7015–33.
45. Song Y, et al. Sirtuin 3-dependent mitochondrial redox homeostasis protects against AGEs-induced intervertebral disc degeneration. Redox Biol. 2018;19:339–53.
46. Newton K, Dixit VM, Kayagaki N. Dying cells fan the flames of inflammation. Science. 2021;374(6571):1076–80.
47. Hoyt LR, et al. Mitochondrial ROS induced by chronic ethanol exposure promote hyper-activation of the NLRP3 inflammasome. Redox Biol. 2017;12:883–96.
48. Tang P, et al. Honokiol alleviates the degeneration of intervertebral disc via suppressing the activation of TXNIP-NLRP3 inflammasome signal pathway. Free Radic Biol Med. 2018;120:368–79.

49. Huang Y, et al. Nicotinamide Phosphoribosyl Transferase Controls NLRP3 inflammasome activity through MAPK and NF-κB signaling in Nucleus Pulposus cells, as suppressed by Melatonin. Inflammation. 2020;43(3):796–809.
50. Yan J, et al. Cholesterol induces pyroptosis and matrix degradation via mSREBP1-Driven endoplasmic reticulum stress in intervertebral disc degeneration. Front Cell Dev Biol. 2021;9:803132.
51. Duan R, Du W, Guo W. EZH2: a novel target for cancer treatment. J Hematol Oncol. 2020;13(1):104.
52. Pan B, et al. SOX4 arrests lung development in rats with hyperoxia–induced bronchopulmonary dysplasia by controlling EZH2 expression. Int J Mol Med. 2017;40(6):1691–8.

Publisher's note